Chapter 2
PB/MPC Navigation Planner

2.1 Introduction

In this chapter, a rather straightforward procedure is presented to obtain navigation algorithms for a broad class of vehicle models, based on an adapted version of the passivity-based nonlinear MPC examined in [1]. The proposed PB/MPC approach for navigation planning can be seen as a generalization of the well-known DWA developed in [2–4]. Similar to the navigation based on the MPC/CLF [5], the PB/MPC optimization setup guarantees the task completion, which means the vehicle is being able to reach the goal position. However, whereas in the MPC/CLF navigation framework a control action that decreases the Lyapunov function has to be found in advance, which is rather difficult if not impossible for complex vehicle models, the PB/MPC navigation framework gives directly the control action as a consequence of the passivity-based control. Therefore, the PB/MPC can be easily adapted to a variety of vehicle and terrain models providing a straightforward procedure for the navigation of wide range of vehicles.

The first step of the procedure requires to shape the energy of the vehicle model by the navigation function which includes information on the goal position and obstacles. A navigation function is constructed for the field or terrain to be traveled in order to shape the energy of the vehicle model including the information on the goal position into the optimization setup. The second step is the selection of the output to force the system to be passive. Passivity-based control is used to make the system equilibrium point globally asymptotically stable, thus guaranteeing task completion.

The obtained properties of the PB/MPC navigation planner can be described as follows. The passivity-based constraint, inherently included in the PB/MPC optimization setup, enhances the navigation by guaranteeing the task completion. In accordance with the MPC paradigm, any additional constraint can be easily imposed into the optimization setup. A general vehicle model is extended by energy-shaping technique using the navigation function, which includes information on the terrain obstacles and the goal position, guaranteeing the avoidance of obstacles while

A. Tahirovic and G. Magnani, *Passivity-Based Model Predictive Control for Mobile Vehicle Motion Planning*, SpringerBriefs in Control, Automation and Robotics,
DOI: 10.1007/978-1-4471-5049-7_2, © The Author(s) 2013

approaching the goal position. Unlike the MPC/CLF navigation framework, where a control action that decreases the value of Lyapunov function has to be found in advance, which is difficult if not impossible for complex vehicle models, the proposed PB/MPC framework gives a control action for any kind of vehicle and terrain models as a consequence of the passivity-based control. Therefore, the PB/MPC approach can be used also for mobile vehicles traveling in outdoor rough terrains, whose behavior is described by truly complex models.

2.2 PB/MPC Optimization Framework

The passivity-based nonlinear control approach, introduced in [1], has been exploited to propose a new mobile vehicle navigation framework for flat terrains [6, 7]. In addition, the PB/MPC navigation framework is extended from flat to rough terrains in [8]. The PB/MPC motion planning optimization framework can be described by the following optimization setup (2.1–2.9):

$$J(\mathbf{u}, \mathbf{r}(x_0)) = \int_{t_0}^{t_0+T} \gamma(\mathbf{x}, \mathbf{u})\mathrm{d}t + \Gamma(t_0 + T), \tag{2.1}$$

$$V(\mathbf{x}) = k\mathrm{NF}(\mathbf{r}) + \frac{1}{2}v^2, \tag{2.2}$$

$$\frac{\mathrm{d}}{\mathrm{d}t}\mathbf{x} = f(\mathbf{x}) + g(\mathbf{x})\mathbf{u} \tag{2.3}$$

$$\mathbf{y} = h(\mathbf{x}) = \left[\frac{\partial V}{\partial x} g(\mathbf{x})\right]^T, \tag{2.4}$$

$$\mathbf{u}^T(t)\mathbf{y}(t) < -\mathbf{y}^T(t)\phi(\mathbf{y}) \tag{2.5}$$

$$\tau : [0, 1] \to C_{\mathrm{free}}, \tau(0) = \mathbf{q}(t_0), \tau(1) = \mathbf{q}(t_0 + T) \tag{2.6}$$

$$v(t_0 + T) = 0 \tag{2.7}$$

$$\begin{aligned} \cos\angle(\nabla\mathrm{NF}, \mathbf{e}_{\dot{r}})|_{t=t_0+T_1} &< 0 \\ \cos\angle(\nabla\mathrm{NF}, \mathbf{e}_{\dot{r}})|_{t=t_0+T} &< 0 \end{aligned} \tag{2.8}$$

$$\mathrm{NF}(\mathbf{r}(t_0 + T)) < \mathrm{NF}(\mathbf{r}(t_0 + T_1)) < \mathrm{NF}(\mathbf{r}(t_0)) \tag{2.9}$$

The main difference between the PB/MPC planners for flat and for rough terrains is in the cost function (2.1). In addition, the last constraint (2.9) is not necessarily required for the PB/MPC planner for flat terrains. These differences will be explained in the sequel to the chapter.

2.2.1 Cost Function

The task of this optimization is to find such a control input $\mathbf{u}$ to guide the vehicle (traction force and steering angle momentum) for each optimization time horizon $t \in (t_0, t_0 + T)$, over all potential alternatives, by minimizing the cost function $J(\mathbf{u})$ given in (2.1). The integrand $\gamma(\mathbf{x}, \mathbf{u})$ is selected depending on what is locally required to minimize. The term $\Gamma(t_0 + T)$ represents an estimation of the cost-to-go value with respect to the goal position in terms of selected measure.

For the PB/MPC motion planner on flat terrains, the cost function is selected to be the value of the energy storage function at the end of the optimization horizon

$$J(\mathbf{u}) = V(\mathbf{x}(t_0 + T)), \tag{2.10}$$

where function $V(\mathbf{x})$ is selected as in (2.2). It includes a virtual potential term constructed by the navigation function of the given terrain, $\mathrm{NF}(\mathbf{r})$ [9, 10], which is selected to have a unique minimum at the goal position, and a kinetic term, $\frac{1}{2}v^2$, where $\mathbf{r} = (x_{cg}, y_{cg})$ and v are the current vehicle coordinates and velocity. The concept of the navigation function has been rigorously introduced in [11]. The main motive behind the construction of such a function is the problem of the local minima which inherently appear in potential fields functions [12]. In [11], the authors have found the exact analytical expressions to construct a function which includes all terrain obstacles while having only a global minimum in the goal position. Some numerical solutions to the same problem has been given in [9, 10], where the navigation function might be expressed as being the shortest paths from each cell of a grid terrain to the goal position. The numerical navigation function given in [9] (NF1), is used in this work. The $\mathrm{NF}(\mathbf{r})$ function is computed for each point of a rectanguloid grid, which is made by appropriate terrain map discretization, as the $\mathcal{L}^1$ (Manhattan) distance to the goal position. In such a case, $\mathrm{NF}(\mathbf{r})$ function approximately represents the shortest path to the goal from each obstacle-free terrain point. This choice assures $\mathrm{NF}(\mathbf{r})$ has a unique minimum at the goal position. A numerical navigation function is not a differentiable function which might cause some problems while using algorithms to solve optimal control problems. The problem of differentiability of a numerical function will be addressed in Chap. 4 under Sect. 4.3.

Since the navigation function has a unique minimum at the goal position [9], the energy storage function given by (2.2) has a unique global minimum at $(x_{cg}\ y_{cg}\ v) = (x_{goal}\ y_{goal}\ 0)$. Hence, by decreasing the objective function (2.10), the vehicle gradually approaches the goal position by choosing the shortest possible paths while satisfying the PB/MPC optimization constraints (2.3–2.9). V follows the definition of the CLF used in the MPC/CLF paradigm proposed in [5] for the particular problem of the navigation of the unicycle mobile robot in flat terrain.

However, choosing the shortest path to the goal position may be a rather strict constraint especially when the vehicle moves in rough terrains. A natural choice of the cost function (2.1) for the PB/MPC planner on rough terrains is a roughness measure computed along the path to be traversed. For this purpose, we introduce some possible cost functions that can describe the roughness level, or traversability index, along the selected path. The first candidate for a cost measure is a function that penalizes high roll and pitch values along the path. Such a function is used in [13] and is given by

$$\gamma(\mathbf{x}, \mathbf{u}) = (1 + \alpha(\varphi^2 + \theta^2)), \tag{2.11}$$

where φ, θ are the roll and pitch angles of the vehicle along the candidate path. Coefficient α represents the tradeoff between the minimum-time and minimum slope-dwell solutions. If $\alpha = 0$, then the solution gives the fastest path within the horizon.

A second candidate was proposed in [14] and is given by

$$\gamma(\mathbf{x}, \mathbf{u}) = \frac{1}{v_{\max}(\mathbf{r})}. \tag{2.12}$$

This function describes the roughness level in terms of the high mobility of the vehicle, where $v_{\max}(\mathbf{r})$ is the predicted maximal value of the vehicle velocity at each position $\mathbf{r}(t)$, $\forall t \in (t_0, t_0 + T)$, along a candidate path, which still does not cause sideslip and rollover of the vehicle [15, 16]. This function is more descriptive when it is important to increase the vehicle mobility. It favors those paths that allow high speeds while preserving the vehicle stability constraints.

Other possibilities for the estimation of the roughness measures along a candidate path are given in [17–19], where the authors introduced a traversability index describing the roughness of the terrain. Regardless of the choice of the measure, the vehicle prefers to find smoother regions toward the goal position, since all the aforementioned measures represent a kind of traversability index along a candidate path considered within the optimization.

For demonstration purposes, a local measure of the roughness is estimated by the relative height of the terrain describing its deviation from flatness and is given by

$$\gamma(\mathbf{x}, \mathbf{u}) = \frac{\sqrt{\mathrm{var}(z(\mathcal{R}))}}{d}, \tag{2.13}$$

where d is the vehicle wheel diameter scaling the selected roughness measure to vehicle size, and $\sqrt{\mathrm{var}(z(\mathcal{R}))}$ being the standard deviation of the terrain height, $z(\mathcal{R})$, along a candidate path, where $\mathcal{R}$ is a terrain map [20]. This approximation is done for all candidate paths within the optimization horizon. However, the approach remains general since any aforementioned roughness functions can be used.

The proposed algorithm optimizes the roughness level toward the goal position in order to select smoother paths. To this purpose, the cost-to-go term $\Gamma(t_0 + T)$ representing the roughness-to-go value at the end of the optimization horizon, is added to the locally used roughness measure, in accordance with (2.1). The estimation of the optimal cost-to-go value within a nonlinear MPC framework is often impossible, and some rough estimations have to be found. Obtaining the optimal cost-to-go map for each terrain location is also likely impossible especially for the problems of the vehicle navigation on large-scale rough terrains. The reason is that the differential constraints have to be taken into account starting from each vehicle initial configuration. One way to construct a numerical roughness-based navigation function for the purpose of an MPC-like motion planning has been presented in [21, 22]. In addition, every time new information is acquired by the vehicle, the update procedure of the **D*** algorithm [23, 24] can be used to get the updated cost-to-go map. Obtaining a differentiable objective function required to solve the optimization problem is addressed in Chap. 4 under Sect. 4.3.

Finally, the choice of the optimization and control horizon design parameters, T and T_1, can influence the final result. The control horizon, T_1, can be a sample cycle period as in most MPC schemes, while the choice of T can be further analyzed. However, regardless of the choice of these parameters, we assume only that $L_{\max} \geq T \cdot v_{\max}$, where $L_{\max}$ is the maximum radius of the visible region with respect to the vehicle current position, and $v_{\max}$ being the vehicle maximum velocity.

2.2.2 Optimization Constraints

Equation (2.3) represents the virtual model obtained by shaping the energy of the real vehicle dynamics by the navigation function, where $\mathbf{x}$ are the new states. The choice of the output (2.4) forces the system to be passive with respect to a radially unbounded and continuously differentiable storage function V, and is based on the passivity control concept.

Passivity constraint (2.5), where ϕ represents a damping injected to the model, asymptotically stabilizes the goal position providing the decrease of the energy storage function V.

Equation (2.6) constrains the optimization to the collision-free configurations, where τ is the map from the initial to the final vehicle configuration $\mathbf{q}$, into the collision-free space C_{free}. Constraint (2.7) guarantees that the selected control $\mathbf{u}$ can stop the vehicle at the end of the horizon satisfying collision-free constraint (2.6). If this constraint holds, then any state space point $\mathbf{x}(T_1)$ preserves the safe policy, where $T_1 < T$. The optimization preformed for the horizon T repeats each T_1.

The conditions given in (2.8), where $\angle(\nabla \text{NF}, \mathbf{e}_{\dot{r}})$ is the current angle between the gradient of the navigation function and the current vehicle velocity direction $\dot{\mathbf{r}}$ represented by its unit vector $\mathbf{e}_{\dot{r}}$, are the terminal conditions which keep the vehicle oriented toward the decrease of the navigation function at the end of each PB/MPC optimization cycle. This constraint guarantees that the energy-shaped system includes some properties providing the asymptotic stability of the system [6].

The passivity constraint (2.5) ensures the decrease of the energy storage function V. This does not ensure the decrease of the virtual potential term NF (2.2) of V at any time within the optimization horizon because of the kinetic energy term $\frac{1}{2}v^2$. As it was already discussed the choice of the objective function given in (2.10) yields the minimization of the value of the navigation function at the end of each optimization horizon. Such optimization policy aims at generating paths toward the steepest descent of the navigation function surface assuring the orientation of the vehicle to be toward its decrease. In case a cost function different from (2.10) is used, in such cases of rough terrains, an additional constraint must be imposed into the PB/MPC framework given by (2.9) to ensure the decrease of the navigation function along the selected paths. Since the optimization is performed within the time T while the control action $\mathbf{u}$ is applied each time T_1, both conditions of (2.9) need to be included.

In addition to the constraints given by Eqs. (2.3–2.9), any additional constraints such as the control input limitations (e.g., maximum velocity), preventing the vehicle from the rolling over or from the slippage, can be easily included into the optimization setup.

2.2.3 Optimization Techniques

The MPC optimization can be conducted by a discrete number of motion primitives using the extreme-left, left, straight, right, and the extreme-right maneuvers which use the maximum acceleration allowed within a particular time horizon by the PB/MPC navigation scheme in accordance with the expression derived later (3.36). However, the MPC optimization problem can be solved by parameterization of the control space within the given horizon as it is nicely demonstrated in [13], when the optimization is solvable by a nonlinear programming optimization technique. Another approach based on a priori defined motion primitives that has widely been used in mobile vehicle navigation [25], was also used in [26]. In [6], the genetic algorithm (GA) is implemented for the local optimization as an alternative to the optimization approach based on defined motion primitives, where chromosomes consisted of the potential values of the vehicle accelerations and steering angles. Such optimizations provide more efficient ways of covering the vehicle control space improving the final solution. However, another way of tackling the local environment constraints that can be used instead of control space sampling is the vehicle state space sampling of feasible motions as discussed and illustrated in [27]. A reader can find a comprehensive overview of different optimization techniques used for the vehicle navigation in [27]. The possible implementation of an MPC-like motion planning algorithm using an optimal control software is presented in Chap. 4 under Sect. 4.3. Therein, a possible lack of a feasible solution for an optimization cycle is addressed by introducing an alternative motion strategy to keep the vehicle moving forward. Such a backup strategy can also be used as a candidate control by the GA algorithm in order to avoid the problem of not finding a feasible solution by the MPC-like optimization framework. Results suggest that both a GA and an optimal control software can be used to solve the optimization setup given by Eqs. (2.1–2.9).

As an example, Fig. 2.1 shows the block diagram of the PB/MPC motion planning approach for rough terrains. The '**Energy-shaped Virtual Model**' and '**Constraint I: Passivity based**' blocks are used to shape the energy of the system and to obtain a passive system, (2.2–2.5). The '**Constraint II: Steering**' block provides the feasible set of steering angles (or steering momenta) $\mathbf{U}_s$, where $u_s \in \mathbf{U}_s$. The '**Constraint III:**

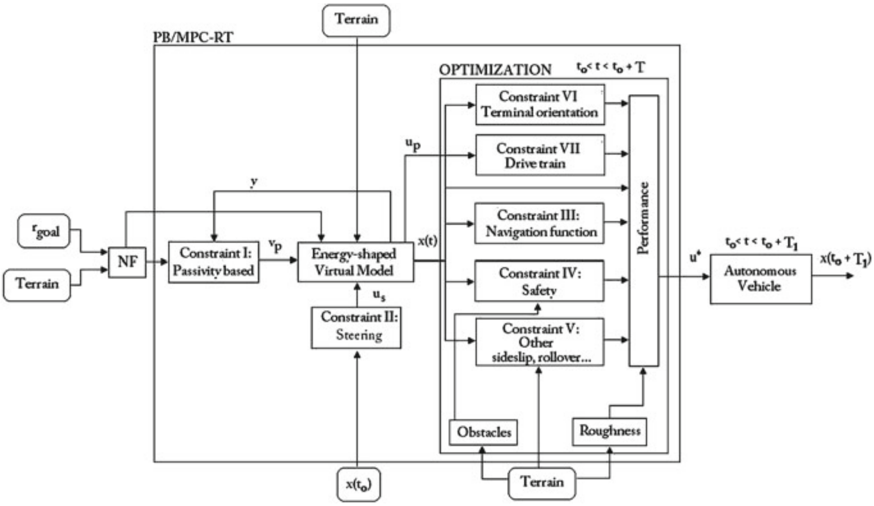

Fig. 2.1 Block diagram of the PB/MPC navigation approach for rough terrains

Navigation function' and '**Constraint IV: Safety**' blocks check for the constraint on decrease of the navigation function (2.9) and the safety conditions (2.6, 2.7), respectively. The '**Constraint V**' block may include some additional constraints related to the vehicle stability conditions such as sideslip and rollover. These constraints estimate the maximum admissible vehicle velocity profile along a candidate path that still does not cause sideslip or rollover of the vehicle. The passivity-based constraint (2.5) provides the feasible set $\mathbf{V}_p$ for the new traction force input $v_p \in \mathbf{V}_p$. The traction force limitations of the input u_p can be checked using the block '**Constraint VII: Drive Train**' within the optimization. Finally, the block: '**Constraint VI: Terminal Orientation**' is used to force the vehicle to be oriented toward the decrease of the navigation function at the end of each MPC optimization horizon in accordance with (2.8).

2.3 Design of the PB/MPC Motion Planner

2.3.1 General Model

The model of a mobile vehicle driven with the traction force u_p and the steering angle momentum u_s, can be expressed in a rather general form by [28]

$$\dot{x} = f(x) + G(x)(u_p \; u_s)^T, \tag{2.14}$$

where $x \in R^n$ is the vehicle state vector, $x = (x_{\mathrm{cg}}\ y_{\mathrm{cg}}\ v\ x_4\ x_5\ \ldots\ x_n)^T$ and the position of the vehicle center of mass $(x_{\mathrm{cg}}, y_{\mathrm{cg}})$, and the velocity of the vehicle v are the states of interest with respect to the final goal position. $(x_4\ x_5\ \ldots\ x_n)$ are the remaining states (see Chap. 3). The goal of the navigation task can be stated as making $(x_{\mathrm{cg}}\ y_{\mathrm{cg}}\ v)_e = (x^*\ y^*\ 0)$ to be a globally asymptotically stable equilibrium point, being (x^*, y^*) the goal position and $(\cdot)_e$ denoting the equilibrium point of the corresponding subsystem.

In order to have the goal position included in a candidate state for the zero equilibrium point of the subsystem represented by $(x_{\mathrm{cg}}\ y_{\mathrm{cg}}\ v)$, the position coordinates have to be transformed as $e_x = x_{\mathrm{cg}} - x^*$, $e_y = y_{\mathrm{cg}} - y^*$, yielding

$$\dot{e} = f(e) + G(e)(u_p\ u_s)^T, \tag{2.15}$$

where

$$e = (e_x\ e_y\ v\ x_4\ x_5 \ldots x_n)^T,$$

$$f(e) = (vf_{e_x}\ vf_{e_y}\ f_v\ f_{x_4}\ f_{x_5} \cdots f_{x_n})^T,$$

$$G(e) = \begin{pmatrix} g_{e_x1} & g_{e_{y1}} & g_{v1} & g_{41} & g_{51} & \cdots & g_{n1} \\ g_{e_x2} & g_{e_{y2}} & g_{v2} & g_{42} & g_{52} & \cdots & g_{n2} \end{pmatrix}^T.$$

It can be seen that the first two equations in (2.15) carry the information on the vehicle nonholonomic constraint.

2.3.2 Energy-Shaping Using a Navigation Function

In general, the equilibrium point of the subsystem described by $(e_x\ e_y\ v)$ will not be the zero one, that is $(e_x\ e_y\ v)_e \neq (0\ 0\ 0)$, since the system has no global information about the goal position. The traction force input u_p can be selected to shape the energy of the system with an injection of additional information on the exact goal position providing $(e_x\ e_y\ v)_e = (0\ 0\ 0)$ for this purpose. This can be achieved using a navigation function of the given terrain $\mathrm{NF}(\mathbf{r})$ with a unique minimum at the goal position, that is $\min \mathrm{NF}(\mathbf{r}) = \mathrm{NF}(\mathbf{r}^*)$, as the part of the selected traction force input. Many different ways to compute NF are discussed in [9].

It is worth noting that

$$\|\dot{\mathbf{r}}\| = \sqrt{\dot{x_{\mathrm{cg}}}^2 + \dot{y_{\mathrm{cg}}}^2} = \sqrt{\dot{e}_x^2 + \dot{e}_y^2} = vf_r, \tag{2.16}$$

where $f_r = \sqrt{f_{e_x}^2 + f_{e_y}^2}$ is a nonnegative function, since for a general vehicle model and for some $\mathbf{r}$ it may result $f_r \neq 1$, implying $\|\dot{\mathbf{r}}\| \neq v$.

It is assumed that g_{v1} is a nonsingular and positive function for all $x \in R^n$, and that the states of system (2.15) are measured or estimated at the end of each optimization horizon, since the MPC optimization requires the initial values of the states of the reshaped vehicle model for the subsequent optimization cycle. Besides vehicle velocity v, and steering angle δ, usually a SLAM has to be solved to obtain the vehicle position $\mathbf{r}$, and its heading angle ψ. Other vehicle states can be measured by the Inertial Measurement Units and other sensors. In this case, the energy of the system can be shaped taking

$$u_p = g_{v_1}^{-1}(-f_v - k\nabla\,\mathrm{NF}(\mathbf{r})\mathbf{e}_{\dot{r}}\, f_r - g_{v_2}u_s) + v_p, \tag{2.17}$$

where

$$k\nabla\,\mathrm{NF}(\mathbf{r})\mathbf{e}_{\dot{r}} = k\|\nabla\,\mathrm{NF}(\mathbf{r})\|\cos\angle(\nabla\,\mathrm{NF}(\mathbf{r}), \mathbf{e}_{\dot{r}}) \tag{2.18}$$

is the scaled inner product of the gradient of the navigation function NF($\mathbf{r}$) with a unit vector of the current direction represented by vector $\mathbf{e}_{\dot{\mathbf{r}}}$. This term favors those directions that move the vehicle along the paths which decrease the value of the navigation function NF($\mathbf{r}$), hence toward the goal position. For instance, if the vehicle goes in the direction of the steepest descent of the navigation function, (2.18) will have a minimum possible value thus providing the maximum value in (2.17). If the vehicle moves increasing values of the navigation function, the component (2.18) will have positive values, hence decreasing the speed and stopping the vehicle. v_p is the new control input of the system replacing the traction force.

In [4] the authors discussed how to construct the navigation function for the case when the vehicle only has information about its sensor range environment.

Given (2.17), the system (2.15) transforms as

$$\dot{e} = \tilde{f}(e) + \tilde{G}(e)(v_p\ u_s)^T, \tag{2.19}$$

where

$$\tilde{f}(e) = (v\tilde{f}_{e_x}\ v\tilde{f}_{e_y}\ \tilde{f}_v\ \tilde{f}_{x4}\ \tilde{f}_{x5}\ \dots\ \tilde{f}_{x_n})^T,$$
$$\tilde{G}(e) = \begin{pmatrix} g_{e_x1} & g_{e_y1} & g_{v1} & g_{41} & \cdots & g_{n1} \\ \tilde{g}_{e_x2} & \tilde{g}_{e_y2} & \tilde{g}_{v2} & \tilde{g}_{42} & \cdots & \tilde{g}_{n2} \end{pmatrix}^T,$$

and defining

$$g_{11} = g_{e_x1};\ g_{21} = g_{e_y1};\ g_{31} = g_{v1};\quad f_{x1} = vf_{e_x};\ f_{x2} = vf_{e_y};$$
$$g_{12} = g_{e_x2};\ g_{22} = g_{e_y2};\ g_{32} = g_{v2},\quad f_{x3} = f_v,$$

it results

$$\tilde{g}_{i2} = g_{i2} - g_{i1}\frac{g_{v2}}{g_{v1}}, \tag{2.20}$$

$$\tilde{f}_{xi} = f_{xi} + \frac{g_{i1}}{g_{v1}} \left(-f_v - k\nabla \text{NF}(\mathbf{r})\mathbf{e}_{\dot{r}} f_r\right), i = 1, \ldots, n; \tag{2.21}$$

providing $\tilde{g}_{v_2} \equiv 0$, and

$$\dot{v} = -k\nabla \text{NF}(\mathbf{r})\mathbf{e}_{\dot{r}} f_r + g_{v_1} v_p. \tag{2.22}$$

For the sake of consistency of the notation to the passivity based control theory presented in the next section, (2.19) will be denoted as

$$\dot{x} = f(x) + G(x) \begin{pmatrix} v_p \\ u_s \end{pmatrix}. \tag{2.23}$$

Theorem 2 *If the general vehicle dynamic model (2.14) is transformed into (2.15) and the system energy is shaped by (2.17), the subsystem described by the states* $x_{\text{ss}} = (e_x \ e_y \ v)^T$ *of the new vehicle dynamic model (2.19) will have zero equilibrium point, that is* $x_{\text{ss}} = 0$.

Proof Assuming $\dot{e}_x = 0$, $\dot{e}_y = 0$ and $\dot{v} = 0$, namely that there is no movement in both directions of the reference frame, the vehicle velocity is equal to zero, $v = 0$. From $\dot{v} = 0$, using (2.22) with input $v_p \equiv 0$, it follows $\nabla \text{NF}(\mathbf{r})\mathbf{e}_{\dot{r}} = 0$. One possible solution of the latter equation, $\cos(\nabla \text{NF}(\mathbf{r})\mathbf{e}_{\dot{r}})) = 0$, implies that the first condition in (2.8) is not satisfied for the given assumptions since this equality then also holds at the end of the operating time horizon T_1. This means that the feasible solution to this equation is only $\mathbf{r} = (x^* \ y^*)$, that is, $e_x = 0$ and $e_y = 0$, since the unique minimum of the navigation function $\text{NF}(\mathbf{r})$ is at this point.

2.3.3 *Energy Storage Function*

The main task of the navigation planning algorithm is to generate reference trajectories using the energy shaped model of the vehicle, whose subsystem consisting of the states of interest has an equilibrium point $x_{\text{ss}} = 0$. In order to find the inputs that move the vehicle toward the goal position, an appropriate energy storage function has to be selected. In [5] the authors used the direct Control Lyapunov function approach in order to navigate the unicycle mobile vehicle. The MPC/CLF optimization setup has the explicit constraint on the decrease of Lyapunov function along trajectories of the system, that is, $\dot{V} \leq -\epsilon\sigma(x)$, where the function $\epsilon\sigma(x)$ is a properly selected positive definite function. In order to satisfy this constraint, one should find such control action to make the system stable. For a unicycle mobile vehicle, the stabilizing control actions can be easily found as illustrated in [5]. Although there are some procedures to obtain stabilizing control actions using given Lyapunov function for particular class of systems, this is generally a hard task for many nonlinear systems.

Since in (2.19) a potential energy term exists in the form of the navigation function $\text{NF}(\mathbf{r})$, a natural choice of the energy storage function is similar to the one proposed in [5] and given by (2.2). A major difference with respect to the Lyapunov function proposed in [5], where only the unicycle mobile robot was considered, is that in (2.2) a distinction is made between $\|\dot{\mathbf{r}}\|$ and v, which is necessary for more accurate car-like vehicle models (see Eq. (2.16)). With the assumption that the navigation function $\mathrm{NF}(\mathbf{r})$ can be constructed such that it is continuously differentiable, and since this storage energy function $V(x)$ is clearly radially unbounded and positive definite, this choice of $V(x)$ satisfies condition (1.5).

From (2.16) and (2.22), it results

$$\begin{aligned}\frac{\partial V}{\partial x} f(x) &= \begin{pmatrix} \frac{\partial V}{\partial \mathbf{r}} & \frac{\partial V}{\partial v} & \frac{\partial V}{\partial x_3} & \cdots & \frac{\partial V}{\partial x_n} \end{pmatrix} f(x) = (k\nabla \mathrm{NF}(\mathbf{r}) \;\; v \;\; \mathbf{0}) f(x) \\ &= k\nabla \mathrm{NF}(\mathbf{r})\dot{\mathbf{r}} + v(-k\nabla \mathrm{NF}(\mathbf{r})\mathbf{e}_{\dot{r}} f_r) = 0, \forall x.\end{aligned} \tag{2.24}$$

2.3.4 Passivity

In order to have a passive system, the output of the system is selected according to (2.4) and is given by

$$\begin{aligned}\mathbf{y}^T &= \begin{pmatrix} \frac{\partial V}{\partial \mathbf{r}} & \frac{\partial V}{\partial v} & \frac{\partial V}{\partial x_3} & \cdots & \frac{\partial V}{\partial x_n} \end{pmatrix} G(x) = (k\nabla \mathrm{NF}(\mathbf{r}) \;\; v \;\; \mathbf{0}) G(x) \Rightarrow \\ \mathbf{y}^T &= (g_{v_1} v \; 0) \Rightarrow y_1 = g_{v_1} v.\end{aligned} \tag{2.25}$$

This means that the output of interest for the given storage function is y_1 that will be used to define a damping feedback to the model, as discussed in subsection 2.3.6, only through input u_p.

2.3.5 Zero State Observability

Theorem 3 *If a general vehicle dynamic model (2.14) is transformed into (2.15) and if its energy shaping form and output are selected as in (2.17) and (2.3.4), respectively, the subsystem described by the three states of interest x_{ss} of the new vehicle dynamic model (2.19) will be zero-state observable.*

Proof This claim is easy to verify starting from the subsystem

$$\begin{pmatrix} \dot{e_x} \\ \dot{e_y} \\ \dot{v} \end{pmatrix} = \begin{pmatrix} v\tilde{f}_{e_x} \\ v\tilde{f}_{e_y} \\ \tilde{f}_v \end{pmatrix} + \begin{pmatrix} g_{e_x 1} & \tilde{g}_{e_x 2} \\ g_{e_y 1} & \tilde{g}_{e_y 2} \\ g_{v1} & \tilde{g}_{v2} \end{pmatrix} \begin{pmatrix} v_p \\ u_s \end{pmatrix}, \tag{2.26}$$

with the condition $y \equiv 0$ and $u \equiv 0$. This implies $v \equiv 0$ since the output is selected as in (2.3.4). This means $\dot{e_x} = 0$ and $\dot{e_y} = 0$, as well as $\dot{v} = 0$. Using (2.22), it follows $\nabla \mathrm{NF}(\mathbf{r})\mathbf{e}_{\dot{r}} = 0$. Similar to the discussion given in the proof of Theorem 2, the latter equation implies $\mathbf{r} = (x^* \ \ y^*)$, that is $e_x = 0$ and $e_y = 0$, so that $x_{\mathrm{ss}} = 0$, namely the subsystem (2.26) is ZSO.

2.3.6 Stability

Since all conditions of Theorem 1 are satisfied, the input v_p can be selected in the form $v_p = -\phi(y)$, where ϕ is any locally Lipschitz function such that $\phi(0) = 0$ and $y^T\phi(y) > 0$ for all $y \neq 0$. One possible choice of a damping injection using the function $\phi(y)$ is (see e.g. [29])

$$v_p = -\epsilon \frac{1}{g_{v_1}} \frac{2}{\pi} \arctan(k_v v), \tag{2.27}$$

where ϵ and k_v are positive constants to be selected.

In order to obtain stability, by the assumption $v \geq 0$, one can write

$$v_p \leq -\epsilon \frac{1}{g_{v_1}} \frac{2}{\pi} \arctan(k_v v). \tag{2.28}$$

This choice of v_p satisfies (2.5) making the equilibrium point x_{ss} of subsystem (2.26), globally asymptotically stable.

This claim can be easily verified finding the time derivative of the energy storage function along the trajectories of system (2.19) under condition (2.28). In fact, using (2.22)

$$\begin{aligned}
\dot{V} &= \begin{pmatrix} \frac{\partial V}{\partial \mathbf{r}} & \frac{\partial V}{\partial v} & \frac{\partial V}{\partial x_3} & \cdots & \frac{\partial V}{\partial x_n} \end{pmatrix} \dot{x} = (k\nabla \mathrm{NF}(\mathbf{r}) \ \ v \ \ \mathbf{0})\dot{x} \\
&= k\nabla \mathrm{NF}(\mathbf{r})\dot{\mathbf{r}} + v(-k\nabla \mathrm{NF}(\mathbf{r})\mathbf{e}_{\dot{r}} f_r + g_{v_1} v_p) = g_{v_1} v v_p
\end{aligned}$$

and, under constraint (2.28), the condition on the derivative of the energy storage function along the trajectories of the closed-loop system is obtained as follows:

$$\dot{V} = g_{v_1} v v_p \leq -\epsilon v \frac{2}{\pi} \arctan(k_v v). \tag{2.29}$$

Hence, $\dot{V}$ is negative semidefinite and $\dot{V} = 0$ if and only if $v = 0$. Then, by zero-state observability, $y(t) \equiv 0 \Rightarrow x_{\mathrm{ss}} \equiv 0$. Therefore, according to the invariance principle, the origin of the subsystem represented by x_{ss} is globally asymptotically stable. This means that the energy of the system under control, expressed by the sum of the virtual potential NF($\mathbf{r}$) and of the kinetic energy term $\frac{1}{2}v^2$, will decrease along the trajectories of the controlled system, moving the vehicle toward the goal position.

This result gives the final shape of the traction force u_p given by (2.17) and (2.28), over each MPC optimization horizon.

References

1. T. Raff, C. Ebenbauer, F. Allgoewer, *Nonlinear Model Predictive Control: Passivity-based Approach* (Springer, Berlin, 2007)
2. R. Simmons, The curvature-velocity method for local obstacle avoidance, in *Proceedings of the IEEE International Conference on Robotics and Automation*, 1996, pp. 3375–3382
3. D. Fox, W. Burgard, S. Thrun, The dynamic window approach to collision avoidance. IEEE Robot. Autom. Mag. **4**, 23–33 (1997)
4. O. Brock, O. Khatib, High-speed navigation using the global dynamic window approach, in *Proceedings of the IEEE International Conference on Robotics and Automation*, vol. 1. 1999, pp. 341–346
5. P. Oegren, N.E. Leonard, A convergent dynamic window approach to obstacle avoidance. IEEE Trans. Robot. **21**(2), 188–195 (2005)
6. A. Tahirovic, G. Magnani, P. Rocco, Mobile robot navigation using passivity-based MPC, in *Proceedings of the IEEE/ASME International Conference on Advanced Intelligent, Mechatronics*, July 2010, pp. 248–488
7. A. Tahirovic, G. Magnani, General framework for mobile robot navigation using passivity-based MPC. IEEE Trans. Autom. Control **56**(1), (2011)
8. A. Tahirovic, G. Magnani, Passivity-based model predictive control for mobile robot navigation planning in rough terrains, in *Proceedings of the 2010 IEEE/RSJ International Conference on Intelligent Robots and Systems*, Oct 2010
9. J. Latombe, *Robot Motion Planning* (Kluwer, Boston, 1991)
10. J. Barraquand, B. Langlois, J. Latombe, Numerical potential field techniques for robot path planning. IEEE Trans. Syst. Man Cybern. **22**(2), 224–241 (1992)
11. E. Rimon, D.E. Koditschek, Exact robot navigation using artificial potential fields. IEEE Trans. Robot. Autom. **8**, 501–518 (Oct. 1992)
12. O. Khatib, Real-time obstacle avoidance for manipulators and mobile robots. Int. J. Robot. Res. **5**(1), 90–98 (1986)
13. T.M. Howard, A. Kelly, Optimal rough terrain trajectory generation for wheeled mobile robots. Int. J. Robot. Res. **26**(2), 141–166 (2007)
14. K. Iagnemma, S. Shimoda, Z. Shiller, Near-optimal navigation of high speed mobile robots, in *Proceedings of the IEEE/RSJ International Conference on Intelligent Robots and Systems*, vol. 2. 2008, pp. 22—26
15. Z. Shiller, Y.-R. Gwo, Dynamic motion planning of autonomous vehicles. IEEE Trans. Robot. Autom. **7**(2), 241–249 (1991)
16. Z. Shiller, Obstacle traversal for space exploration, in *Proceedings of the IEEE International Conference on Robotics and Automation*, 2000
17. S. Singh, R. Simmons, T. Smith, A. Stentz, V. Verma, A. Yahja, K. Schwehr, Recent progress in local and global traversability for planetary rovers, in *Proceedings of the IEEE International Conference on Robotics and Automation*, 2000
18. H. Seraji, Fuzzy traversability index: a new concept for terrain-based navigation. J. Robot. Syst. **17**(2), 75–91 (2000)
19. A. Howard, H. Seraji, Vision-based terrain characterization and traversability assessment. J. Robot. Syst. **18**(10), 577–587 (2001)
20. K. Iagnemma, S. Dubowsky, *Mobile Robots in Rough Terrain: Estimation, Motion Planning and Control with Application to Planetary Rovers* (Springer, Berlin, 2004)

21. A. Tahirovic, G. Magnani, A roughness-based RRT for mobile robot navigation planning, in *Proceedings of the 18th IFAC World Congress*, 2011, pp. 5944–5949
22. A. Tahirovic, G. Magnani, Y. Kuwata, An approximate of the cost-to-go map on rough terrains, in *Proceedings of the IEEE International Conference on Mechatronics*, 2013
23. A. Stentz, The focussed D* algorithm for real-time replanning, in *Proceedings of the International Joint Conference on Artificial Intelligence*, pp. 1652–1659, 1995
24. S. Koenig, M. Likhachev, Fast replanning for navigation in unknown terrain. IEEE Trans. Robot. **21**(3), 354–363 (2005)
25. A. Lacaze, Y. Moscovitz, N. Declaris, K. Murphy, Path planning for autonomous vehicle driving over rough terrain, in *Proceedings of the IEEE International Symposium on Intelligent Control* (Gaithersburg, MD, 1998), pp. 50–55
26. M. Pivtoraiko, R.A. Knepper, A. Kelly, Differentially constrained mobile robot motion planning in state lattices. J. Field Robot. **26**(3), 308–333 (2009)
27. T.M. Howard, C.J. Green, A. Kelly, D. Ferguson, State space sampling of feasible motions for high-performance mobile robot navigation in complex environments. J. Field Robot. **25**(10), 325–345 (2008)
28. Y. Yoon, J. Shin, H.J. Kim, Y. Park, S. Sastry, Model-predictive active steering and obstacle avoidance for autonomous ground vehicles. Control Eng. Pract. **17**(7), 741–750 (2009)
29. H.K. Khalil, *Nonlinear Systems*, 3rd edn. (Prentice Hall, Upper Saddle River, 2002)

http://www.springer.com/978-1-4471-5048-0

Passivity-Based Model Predictive Control for Mobile Vehicle Motion Planning

Tahirovic, A.; Magnani, G.

2013, XI, 56 p. 20 illus., 17 illus. in color., Softcover
ISBN: 978-1-4471-5048-0